Synchronverters: Inverters That Mimic Synchronous Generators

Qing-Chang Zhong, *Senior Member, IEEE*, and George Weiss

***Abstract*—In this paper, the idea of operating an inverter to mimic a synchronous generator (SG) is motivated and developed. We call the inverters that are operated in this way synchronverters. Using synchronverters, the well-established theory/algorithms used to control SGs can still be used in power systems where a significant proportion of the generating capacity is inverter-based. We describe the dynamics, implementation, and operation of synchronverters. The real and reactive power delivered by synchronverters connected in parallel and operated as generators can be automatically shared using the well-known frequency- and voltage-drooping mechanisms. Synchronverters can be easily operated also in island mode, and hence, they provide an ideal solution for microgrids or smart grids. Both simulation and experimental results are given to verify the idea.**

***Index Terms*—Distributed generation, frequency drooping, inverter-dominated power system, load sharing, microgrid, parallel inverters, pulsewidth modulation (PWM) inverter, renewable energy, smart grid, static synchronous generator (SG), synchronverter, virtual SG, voltage drooping.**

I. Introduction

FOR ECONOMIC, technical, and environmental reasons, the share of electrical energy produced by distributed energy sources, such as combined heat and power (CHP) plants, and renewable-energy sources, such as wind power, solar power, wave and tidal power, etc., is steadily increasing. The European Union has set a 22% target for the share of renewable-energy sources and an 18% target for the share of CHP in electricity generation by 2010. The electrical power system is currently undergoing a dramatic change from centralized generation to distributed generation. Most of these distributed/renewable-energy generators comprise variable-frequency ac sources, high-frequency ac sources, or dc sources, and hence, they need dc–ac converters, also called inverters, to interface with the public-utility grid. For example, wind turbines are most effective if free to generate at variable frequency, and so, they require conversion from variable frequency ac to dc to ac; small gas-turbines with direct-drive generators operate at high frequency and also require ac to dc to ac conversion; photovoltaic arrays require dc–ac conversion. This means that more and more inverters will be connected to the grid and will eventually dominate power generation.

The current paradigm in the control of wind- or solar-power generators is to extract the maximum power from the power source and inject them all into the power grid (see, for example, [1]–[3]). Advanced algorithms have been developed to ensure that the current injected into the grid is clean sinusoidal (see, for example, [4]). The policy of injecting all available power to the grid is a good one as long as renewable power sources constitute a small part of the grid power capacity. Indeed, any random power fluctuation of the renewable power generators will be compensated by the controllers associated with the large conventional generators, and some of these generators will also take care of the overall power balance, system stability, and fault ride through.

When renewable power generators (particularly the solar ones) will provide the majority of the grid power, such "irresponsible" behavior (on their part) will become untenable. Thus, the need will arise to operate them in the same way as conventional power generators or at least to imitate certain aspects of the operation of conventional generators using novel techniques (see [5]–[11]). This will require high-efficiency energy-storage units so that the random fluctuations of the prime power source can be filtered out. The key problem here is how to control the inverters in distributed power generators. There are two options: The first is to redesign the whole power system and to change the way it is operated (e.g., establish fast communication lines between generators and possibly central control) and the second is to find a way so that these inverters can be integrated into the existing system and behave in the same way as large synchronous generators (SG) do. We think that the second option has the advantages, as it would assure a smooth transition to a grid dominated by inverters.

In this paper, we propose a method by which an inverter can be operated to mimic the behavior of an SG. The dynamic equations are the same; only the mechanical power exchanged with the prime mover (or with the mechanical load, as the case may be) is replaced with the power exchanged with the dc bus. We call such an inverter (including the filter inductors and capacitors) and the associated controller a *synchronverter*. To be more precise, a synchronverter is equivalent to an SG with a small capacitor bank connected in parallel to the stator

Manuscript received October 20, 2009; accepted January 19, 2010. Date of publication April 29, 2010; date of current version March 11, 2011. This paper was presented in part at the 2009 IEEE Power Engineering Society Power Systems Conference & Exhibition Seattle, WA, USA, March 2009. The work of Q.-C Zhong was supported in part by the Royal Academy of Engineering, by the Leverhulme Trust, with the award of a Senior Research Fellowship (2009-2010), and by the EPSRC, U.K., with the support of the Network for New Academics in Control Engineering (New Ace, www.newace.org.uk) Grant EP/E055877/1 and the support under the DTA scheme.

Q.-C. Zhong was with the Department of Electrical Engineering and Electronics, University of Liverpool, L69 3GJ Liverpool, U.K. He is now with the Department of Aeronautical and Automotive Engineering, Loughborough University, Leicestershire LE11 3TU, U.K.

G. Weiss is with the Department of Electrical Engineering Systems, Faculty of Engineering, Tel Aviv University, Ramat Aviv 69978, Israel (e-mail: gweiss@eng.tau.ac.il).

Color versions of one or more of the figures in this paper are available online at http://ieeexplore.ieee.org.

Digital Object Identifier 10.1109/TIE.2010.2048839

0278-0046/$26.00 © 2010 IEEE

terminals. A sychronverter will have all the good and bad properties of an SG, which is a complex nonlinear system. For example, the undesirable phenomena, such as loss of stability due to underexcitation as well as hunting (oscillations around the synchronous frequency), could occur in a synchronverter. An advantage is that we can choose the parameters, such as inertia, friction coefficient, field inductance, and mutual inductances. (The energy that would be lost in the virtual mechanical friction is not lost in reality; it is directed back to the dc bus.) Moreover, we can (and do) choose to have no magnetic saturation and no eddy currents. If we want, we can choose parameter values that are impossible in a real SG, and we can also vary the parameters while the system is operating.

If a synchronverter is connected to the utility grid and is operated as a generator, no difference would be felt from the grid side between this system and an SG. Thus, the conventional control algorithms and equipment that have been developed for SGs driven by prime movers (and which have reached a high level of maturity over 100 years) can be applied to synchronverters. Synchronverters can also be operated as synchronous motors based on the same mathematical derivation. One option is to decide the direction of the energy flow between the dc bus and the ac bus in a synchronverter automatically according to the grid frequency. We think that synchronverters operated as synchronous motors will be useful, for example, in high-voltage dc transmission lines, where dc power would be sent from a synchronverter working as a motor to another one working as a generator at the other end of the line.

We mention that IEEE defined a term, called *static SG* [12], to designate a static self-commutated switching power converter supplied from an appropriate electric energy source and operated to produce a set of adjustable multiphase output voltages, which may be coupled to an ac power system for the purpose of exchanging independently controllable real and reactive power. This term was originally defined for one of the shunt-connected controllers in flexible ac transmission system. Clearly, synchronverters operated as generators would be a particular type of static SGs.

There are papers in the literature exploring related ideas. The concept of a *virtual synchronous machine* (VISMA) was proposed in [13], where the voltages at the point of common coupling with the grid are measured to calculate the phase currents of the VISMA in real time. These currents are then used as reference currents for the inverter, and hence, the inverter behaves as a current source connected to the grid. If the current tracking error is small, then the inverter behaves like a synchronous machine, justifying the term VISMA. If the current tracking error is large, then the inverter behavior changes. They provided extensive experimental results (but the grid integration of VISMA using control algorithms for SG was left as future work). As a key difference to the synchronverter, it is worth mentioning that the synchronverter does not depend on the tracking of reference currents or voltages. In [15] and [16], a short-term energy-storage system is added to the inverter in order to provide virtual inertia to the system. The power flow to the storage is proportional to the derivative of the grid frequency (as it would be with real inertia). This kind of inverter with added virtual inertia, called *virtual SGs*, can contribute to the short-term stabilization of the grid frequency. However, the system dynamics seen from the grid side will be different from those of an SG.

The rest of this paper is organized as follows. In Section II, a dynamic model of SGs is established under no assumptions on the signals. Although the model of an SG is well documented in the literature, the way the model is described here is somewhat fresh. The way to implement a synchronverter is described in Section III, and issues related to its operation, e.g., frequency- and voltage-drooping mechanisms for load sharing, are described in Section IV. Simulation results are given in Section V, and experimental results are given in Section VI with conclusions in Section VII. A patent application has been filed for the technology described here.

II. Modeling Synchronous Machines

The model of synchronous machines can be found in many sources such as [17]–[21]. Most of the references make various assumptions, such as steady state and/or balanced sinusoidal voltages/currents, to simplify the analysis. Here, we briefly outline a model that is a (nonlinear) passive dynamic system without any assumptions on the signals, from the perspective of system analysis and controller design. We consider a round rotor machine so that all stator inductances are constant. Our model assumes that there are no damper windings in the rotor, that there is one pair of poles per phase (and one pair of poles on the rotor), and that there are no magnetic-saturation effects in the iron core and no eddy currents. As is well known, the damper windings help to suppress hunting and also help to bring the machine into synchronism with the grid (see, for example, [21]). We leave it for later research to establish if it is worthwhile to include damper windings in the model used to implement a synchronverter. Our simulation and experimental results do not seem to point at such a need-we got negligible hunting, and we got fast synchronization algorithms without using damper windings.

A. Electrical Part

For details on the geometry of the windings, we refer to [18] and [19]. The field and the three identical stator windings are distributed in slots around the periphery of the uniform air gap. The stator windings can be regarded as concentrated coils having self-inductance L and mutual inductance $-M$ ($M > 0$ with a typical value $1/2L$, the negative sign is due to the $2\pi/3$ phase angle), as shown in Fig. 1. The field (or rotor) winding can be regarded as a concentrated coil having self-inductance L_f. The mutual inductance between the field coil and each of the three stator coils varies with the rotor angle θ, i.e.,

$$M_{af} = M_f \cos(\theta)$$

$$M_{bf} = M_f \cos\left(\theta - \frac{2\pi}{3}\right)$$

$$M_{cf} = M_f \cos\left(\theta - \frac{4\pi}{3}\right)$$

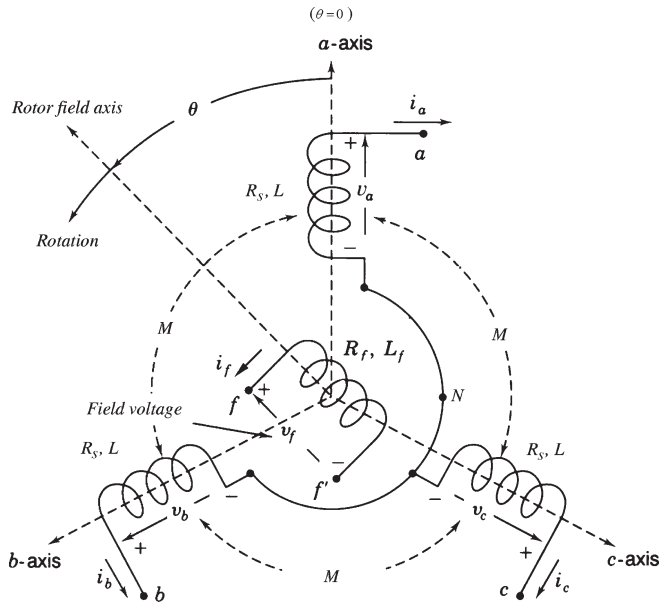

Fig. 1. Structure of an idealized three-phase round-rotor SG, modified from [17, Fig. 3.4].

where $M_f > 0$. The flux linkages of the windings are

$$\begin{aligned}\Phi_a &= Li_a - Mi_b - Mi_c + M_{af}i_f\\ \Phi_b &= -Mi_a + Li_b - Mi_c + M_{bf}i_f\\ \Phi_c &= -Mi_a - Mi_b + Li_c + M_{cf}i_f\\ \Phi_f &= M_{af}i_a + M_{bf}i_b + M_{cf}i_c + L_f i_f\end{aligned}$$

where i_a, i_b, and i_c are the stator phase currents and i_f is the rotor excitation current. Denote

$$\Phi = \begin{bmatrix}\Phi_a\\ \Phi_b\\ \Phi_c\end{bmatrix} \quad i = \begin{bmatrix}i_a\\ i_b\\ i_c\end{bmatrix}$$

$$\widetilde{\cos}\,\theta = \begin{bmatrix}\cos\theta\\ \cos\left(\theta - \frac{2\pi}{3}\right)\\ \cos\left(\theta - \frac{4\pi}{3}\right)\end{bmatrix} \quad \widetilde{\sin}\,\theta = \begin{bmatrix}\sin\theta\\ \sin\left(\theta - \frac{2\pi}{3}\right)\\ \sin\left(\theta - \frac{4\pi}{3}\right)\end{bmatrix}.$$

Assume for the moment that the neutral line is not connected, then

$$i_a + i_b + i_c = 0.$$

It follows that the stator flux linkages can be rewritten as

$$\Phi = L_s i + M_f i_f \widetilde{\cos}\,\theta \tag{1}$$

where $L_s = L + M$, and the field flux linkage can be rewritten as

$$\Phi_f = L_f i_f + M_f \langle i, \widetilde{\cos}\,\theta\rangle \tag{2}$$

where $\langle\cdot,\cdot\rangle$ denotes the conventional inner product in $\mathbb{R}^3$. We remark that the second term $M_f\langle i, \widetilde{\cos}\theta\rangle$ (called armature reaction) is constant if the three phase currents are sinusoidal (as functions of θ) and balanced. We also mention that $\sqrt{2/3}\langle i, \widetilde{\cos}\theta\rangle$ is called the d-axis component of the current.

Assume that the resistance of the stator windings is R_s; then, the phase terminal voltages $v = [v_a \quad v_b \quad v_c]^T$ can be obtained from (1) as

$$v = -R_s i - \frac{d\Phi}{dt} = -R_s i - L_s\frac{di}{dt} + e \tag{3}$$

where $e = [e_a \quad e_b \quad e_c]^T$ is the back electromotive force (EMF) due to the rotor movement given by

$$e = M_f i_f \dot{\theta}\widetilde{\sin}\,\theta - M_f\frac{di_f}{dt}\widetilde{\cos}\,\theta. \tag{4}$$

The voltage vector e is also called no-load voltage or synchronous internal voltage.

We mention that, from (2), the field terminal voltage is

$$v_f = -R_f i_f - \frac{d\Phi_f}{dt} \tag{5}$$

where R_f is the resistance of the rotor winding. However, we shall not need the expression for v_f because we shall use i_f instead of v_f as an adjustable constant input. This completes the modeling of the electrical part of the machine.

B. Mechanical Part

The mechanical part of the machine is governed by

$$J\ddot{\theta} = T_m - T_e - D_p\dot{\theta} \tag{6}$$

where J is the moment of inertia of all the parts rotating with the rotor, T_m is the mechanical torque, T_e is the electromagnetic toque, and D_p is a damping factor. T_e can be found from the energy E stored in the machine magnetic field, i.e.,

$$\begin{aligned}E &= \frac{1}{2}\langle i, \Phi\rangle + \frac{1}{2}i_f\Phi_f = \frac{1}{2}\langle i, L_s i + M_f i_f \widetilde{\cos}\,\theta\rangle\\ &\quad + \frac{1}{2}i_f\left(L_f i_f + M_f\langle i, \widetilde{\cos}\theta\rangle\right)\\ &= \frac{1}{2}\langle i, L_s i\rangle + M_f i_f\langle i, \widetilde{\cos}\,\theta\rangle + \frac{1}{2}L_f i_f^2.\end{aligned}$$

From simple energy considerations (see, e.g., [18] and [22]) we have

$$T_e = \left.\frac{\partial E}{\partial\theta}\right|_{\Phi,\Phi_f\,\text{constant}}$$

(because constant flux linkages mean no back EMF, all the power flow is mechanical). It is not difficult to verify (using the formula for the derivative of the inverse of a matrix function) that this is equivalent to

$$T_e = -\left.\frac{\partial E}{\partial\theta}\right|_{i,i_f\,\text{constant}}.$$

Thus

$$T_e = -M_f i_f\left\langle i, \frac{\partial}{\partial\theta}\widetilde{\cos}\,\theta\right\rangle = M_f i_f\langle i, \widetilde{\sin}\,\theta\rangle. \tag{7}$$

We mention that $-\sqrt{2/3}\langle i, \widetilde{\sin}\theta\rangle$ is called the q-axis component of the current. Note that if $i = i_0\widetilde{\sin}\varphi$ for some arbitrary angle φ, then

$$T_e = M_f i_f i_0 \langle \widetilde{\sin}\,\varphi, \widetilde{\sin}\,\theta\rangle = \frac{3}{2} M_f i_f i_0 \cos(\theta - \varphi).$$

Note also that if i_f is constant (as is usually the case), then (7) with (4) yields

$$T_e\dot{\theta} = \langle i, e\rangle.$$

C. Provision of Neutral Line

The previous analysis is based on the assumption that the neutral line is not connected. If the neutral line is connected, then

$$i_a + i_b + i_c = i_N$$

where i_N is the current flowing through the neutral line. Then, the formula for the stator flux linkages (1) becomes

$$\Phi = L_s i + M_f i_f \widetilde{\cos}\,\theta - \begin{bmatrix}1\\1\\1\end{bmatrix} M i_N$$

and the phase terminal voltages (3) become

$$v = -R_s i - L_s \frac{di}{dt} + \begin{bmatrix}1\\1\\1\end{bmatrix} M \frac{di_N}{dt} + e$$

where e was given by (4). The other formulas are not affected.

As we have seen, the provision of a neutral line makes the system model somewhat more complicated. However, in a synchronverter to be designed in the next section, M is a design parameter that can be chosen to be zero. The physical meaning of this is that there is no magnetic coupling between the stator windings. This does not happen in a physical SG but can be easily implemented in a synchronverter. When we need to provide a neutral line, it is an advantageous choice to take $M = 0$ as it simplifies the equations. Otherwise, the choice of M and L individually is irrelevant; what matters only is that $L_s = L + M$. In the sequel, the model of an SG consisting of (3), (4), (6), and (7) will be used to operate an inverter as a synchronverter.

III. Implementation of Synchronverter

In this section, the details on how to implement a synchronverter will be described. A simple dc/ac converter (inverter) used to convert dc power into three-phase ac (or the other way round) is shown in Fig. 2. It includes three inverter legs operated using pulsewidth modulation (PWM) and LC filters to reduce the voltage ripple (and hence, the current ripple) caused by the switching. In grid-connected operation, the impedance of the grid should be included in the impedance of the inductors L_g (with series resistance R_g), and then we may consider that after the circuit breaker, we have an infinite bus. The circuit shown in Fig. 2 does not provide a neutral line, but this can be added if needed. The *power part of the synchronverter* is the circuit to the left of the three capacitors, together with the capacitors. If we disregard the ripple, then this part of the circuit will behave like an SG connected in parallel with the same capacitors. The inductors, denoted as L_g, are not part of the synchronverter, but it is useful to have them (for synchronization and power control). It is important to have some energy storage (not shown) on the dc bus (at the left end of the figure) since the power absorbed from the dc bus represents not only the power taken from the imaginary prime mover but also from the inertia of the rotating part of the imaginary SG. This latter component of the power may come in strong bursts, which is proportional to the derivative of the grid frequency.

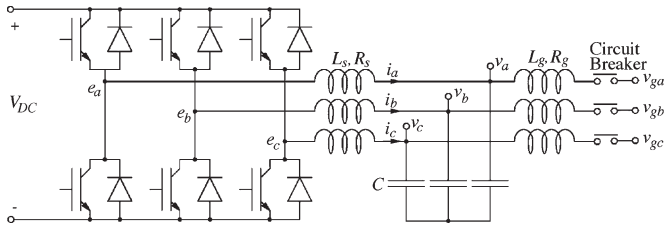

Fig. 2. Power part of a synchronverter—a three phase inverter, including LC filters.

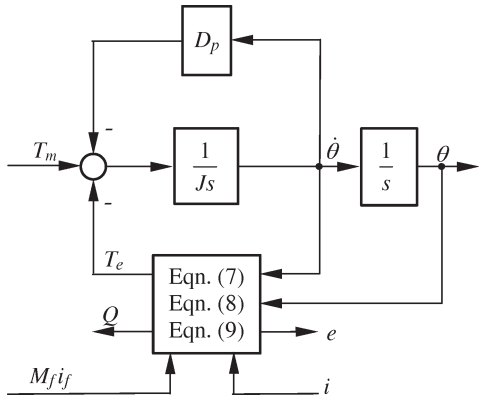

Fig. 3. Electronic part of a synchronverter (without control). This part interacts with the power part via e and i.

What we call the *electronic part of the synchronverter* is a digital signal processor (DSP) and its associated circuits, running under a special program, which controls the switches shown in Fig. 2. Its block diagram is shown in Fig. 3. These two parts interact via the signals e and i (v and v_g will be used for controlling the synchronverter). The various voltage and current sensors and the signal conditioning circuits and analog/digital converters should be regarded as part of the electronic part of the synchronverter. Normally, the program on the DSP will contain also parts that represent the controller of the synchronverter (not the synchronverter itself).

A. Power Part

We give some ideas for the design of the power part. It is important to understand that the terminal voltages $v = [v_a \quad v_b \quad v_c]^T$ of the imaginary SG, as given in (3), are represented by the capacitor voltages shown in Fig. 2. Further,

the impedance of the stator windings of the imaginary SG is represented by the inductance L_s and the resistance R_s of the left inductors shown in Fig. 2. It follows from here that e_a, e_b, and e_c should represent the back EMF due to the movement of the imaginary rotor. This is not possible exactly because e_a, e_b, and e_c are high-frequency switching signals, but it is possible in the average sense: The switches in the inverter should be operated so that the average values of e_a, e_b, and e_c over a switching period should be equal to e given in (4). This can be achieved by the usual PWM technique.

It is advantageous to assume that the imaginary field (rotor) winding of the synchronverter is fed by an adjustable dc current source i_f instead of a voltage source v_f. Then, the terminal voltage v_f varies, but this is irrelevant. As long as i_f is constant, the generated voltage from (4) reduces to

$$e = \dot{\theta} M_f i_f \widetilde{\sin}\,\theta. \tag{8}$$

The filtering capacitors C should be chosen such that the resonant frequency $1/\sqrt{L_s C}$ is approximately $\sqrt{\omega_n \omega_s}$, where ω_n is the nominal angular frequency of the grid voltage and ω_s is the angular switching frequency used to turn on/off the switches (insulated-gate bipolar transistors (IGBTs) are shown in the figure but other power semiconductors can be used as well).

If a neutral line is needed, then the strategies proposed in [23] or [24] to provide a neutral line without affecting the control of the three-phase inverter may be used.

B. Electronic Part

Define the generated real power P and reactive power Q (as seen from the inverter legs) as

$$P = \langle i, e \rangle \quad Q = \langle i, e_q \rangle$$

where e_q has the same amplitude as e but with a phase delayed from that of e by $\pi/2$, i.e.,

$$e_q = \dot{\theta} M_f i_f \widetilde{\sin}\left(\theta - \frac{\pi}{2}\right) = -\dot{\theta} M_f i_f \widetilde{\cos}\,\theta.$$

Then, the real power and reactive power are, respectively

$$\begin{aligned} P &= \dot{\theta} M_f i_f \langle i, \widetilde{\sin}\,\theta \rangle \\ Q &= -\dot{\theta} M_f i_f \langle i, \widetilde{\cos}\,\theta \rangle. \end{aligned} \tag{9}$$

These coincide with the conventional definitions for real power and reactive power, usually expressed in d, q coordinates. Positive Q corresponds to an inductive load. Note that, if $i = i_0 \widetilde{\sin}\varphi$ for some angle φ (this would be the case, e.g., in balanced steady-state operation with $\theta - \varphi$ constant), then

$$\begin{aligned} P &= \dot{\theta} M_f i_f \langle i, \widetilde{\sin}\,\theta \rangle = \frac{3}{2} \dot{\theta} M_f i_f i_0 \cos(\theta - \varphi) \\ Q &= -\dot{\theta} M_f i_f \langle i, \widetilde{\cos}\,\theta \rangle = \frac{3}{2} \dot{\theta} M_f i_f i_0 \sin(\theta - \varphi). \end{aligned}$$

The previous formulas for P and Q are used when regulating the real and reactive power of an SG.

Equation (6) can be written as

$$\ddot{\theta} = \frac{1}{J}(T_m - T_e - D_p \dot{\theta})$$

where the mechanical (or active) torque T_m is a control input, while the electromagnetic torque T_e depends on i and θ according to (7). This equation, together with (7)–(9), is implemented in the electronic part of a synchronverter shown in Fig. 3. Thus, the state variables of the synchronverter are i (the inductor currents), v (the capacitor voltages), θ, and $\dot{\theta}$ (which are a virtual angle and a virtual angular speed). (In the absence of a neutral line, only two of the three currents in the vector i are independent.) The control inputs of the synchronverter are T_m and $M_f i_f$. In order to operate the synchronverter in a useful way, we need a controller that generates the signals T_m and $M_f i_f$ such that system stability is maintained, and the desired values of real and reactive power are followed. The significance of Q will be discussed in the next section.

IV. Operation of Synchronverter

A. Frequency Drooping and Regulation of Real Power

For SGs, the rotor speed is maintained by the prime mover, and it is known that the damping factor D_p is due to mechanical friction. An important mechanism for SGs to share load evenly (in proportion to their nominal load) is to vary the real power delivered to the grid according to the grid frequency, which is a control loop called "frequency droop." When the real-power demand increases, the speed of the SGs drops due to increased T_e in (6). The power regulation system of the prime mover then increases the mechanical power, e.g., by widening the throttle valve of an engine, so that a new power balance is achieved. Typical values for the frequency droop are a 100% increase in power for a frequency decrease between 3% and 5% (from nominal values).

The frequency-droop mechanism can be implemented in a synchronverter by comparing the virtual angular speed $\dot{\theta}$ with the angular frequency reference $\dot{\theta}_r$ (which normally would be equal to the nominal angular frequency of the grid $\dot{\theta}_n$) and adding this difference, multiplied with a gain, to the active torque T_m. The formulas show that the effect of the frequency-droop control loop is equivalent to a significant increase of the mechanical friction coefficient D_p. In Fig. 4 and later, the constant D_p represents the (imaginary) mechanical-friction coefficient plus the frequency-drooping coefficient (the latter is far larger). Thus, denoting the change in the total torque acting on the imaginary rotor by ΔT and the change in angular frequency by $\Delta\dot{\theta}$, we have

$$D_p = -\frac{\Delta T}{\Delta \dot{\theta}}.$$

It is worth noting that, in some references, such as [5], D_p is defined as $-\Delta\dot{\theta}/\Delta T$. Here, the negative sign is to make D_p positive. The active torque T_m can be obtained from the setpoint (or reference value) of the real power P_{set} by dividing it with the nominal mechanical speed $\dot{\theta}_n$, as shown in Fig. 4. (Actually it should be $\dot{\theta}$ instead of $\dot{\theta}_n$, but the relative difference between

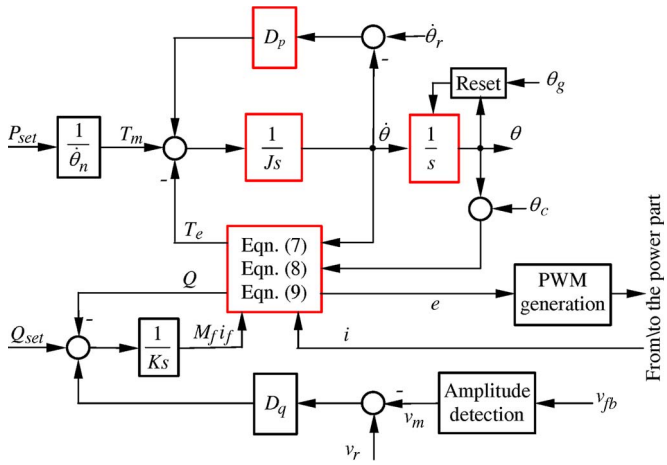

Fig. 4. Regulation of the real and reactive power in a synchronverter.

θ_n and θ is negligible.) This completes the feedback loop for real power, as seen in the upper part of Fig. 4. Because of the built-in frequency-drooping mechanism, a synchronverter automatically shares the load variations with other inverters of the same type and with SGs on the same power grid. The real power regulation loop is very simple because no mechanical devices are involved, and no measurements other than i are needed (all the variables are available in the DSP).

The regulation mechanism of the real power (torque) shown in the upper part of Fig. 4 has a nested structure, where the inner loop is the frequency-droop loop (with feedback gain D_p) and the outer loop is the more complex real power loop (with the feedback coming from the current i via the torque T_e). The time constant of the frequency-droop loop is $\tau_f = J/D_p$. Hence, if we have decided upon τ_f, then J should be chosen as

$$J = D_p \tau_f.$$

Because there is no delay involved in the frequency-droop loop, the time constant τ_f can be made much smaller than for a real SG. It is not necessary to have a large inertia as with a physical SG, where a larger inertia means that more energy is stored mechanically. Whether a small inertia is good for overall grid stability is an open question for later research. At any rate, the energy-storage function of a synchronverter can, and should, be decoupled from the inertia (unlike the approach proposed in [15]). The short-term energy-storage function (inertia) can be implemented with a synchronverter using the same storage system (e.g., batteries) that is used for long-term storage.

B. Voltage Drooping and Regulation of Reactive Power

The regulation of reactive power Q flowing out of the synchronverter can be realized similarly. Define the voltage-drooping coefficient D_q as the ratio of the required change of reactive power ΔQ to the change of voltage Δv, i.e.,

$$D_q = -\frac{\Delta Q}{\Delta v}.$$

We note that in some references (e.g., [5]), D_q is defined as $-\Delta v/\Delta Q$. The control loop for the reactive power can be realized as shown in the lower part of Fig. 4. The difference between the reference voltage v_r and the amplitude v_m of the feedback voltage v_{fb} (normally v_{fb} would be v_g from Fig. 2 if it is available, otherwise, something close to it) is the voltage amplitude tracking error. This error is multiplied with the voltage-drooping coefficient D_q and then added to the tracking error between the reference value $Q_{\rm set}$ and the reactive power Q, which is calculated according to (9). The resulting signal is then fed into an integrator with a gain $1/K$ to generate $M_f i_f$. It is important to note that there is no need to measure the reactive power Q, as it can be computed from i (which is measured) and from θ and $\dot{\theta}$, which are available internally in the DSP.

The control of the reactive power shown in the lower part of Fig. 4 also has a nested structure, if the effect of the LC filter is ignored (which means considering $v_{fb} \approx e$ so that $v_m \approx \dot{\theta} M_f i_f$). The inner loop is the (amplitude) voltage loop, and the outer loop is the reactive-power loop. The time constant τ_v of the voltage loop can be estimated as

$$\tau_v \approx \frac{K}{\dot{\theta} D_q} \approx \frac{K}{\dot{\theta}_n D_q}$$

as the variation of $\dot{\theta}$ is very small. Hence, K follows if τ_v and D_q have been chosen.

The amplitude detector in Fig. 4 can be realized in several ways. One is by using a phase-locked loop (PLL); we do not go into the details of this. Another elementary method is as follows: Assume that $v_{fba} = v_m \sin\theta_a$, $v_{fbb} = v_m \sin\theta_b$, and $v_{fbc} = v_m \sin\theta_c$, then

$$\begin{aligned} &v_a v_b + v_b v_c + v_c v_a \\ &\quad = v_m^2 [\sin\theta_a \sin\theta_b + \sin\theta_b \sin\theta_c + \sin\theta_c \sin\theta_a] \\ &\quad = \frac{v_m^2}{2} [\cos(\theta_a - \theta_b) + \cos(\theta_b - \theta_c) + \cos(\theta_c - \theta_a)] \\ &\qquad - \frac{v_m^2}{2} [\cos(\theta_a + \theta_b) + \cos(\theta_b + \theta_c) + \cos(\theta_c + \theta_a)]. \end{aligned}$$

When the terminal voltages are balanced, i.e., when $\theta_b = \theta_a - 2\pi/3 = \theta_c + 2\pi/3$, then the last term of the aforementioned is zero, and we obtain

$$v_a v_b + v_b v_c + v_c v_a = -\frac{3}{4} v_m^2.$$

The amplitude v_m can be computed from here with ease. In a real implementation, a low-pass filter is needed to attenuate the ripples in v_m (at twice the grid frequency) as the terminal voltages may be unbalanced. This observation applies also to T_e and Q.

V. Simulation Results

The ideas described earlier have been verified with simulations. The parameters of the inverter used in the simulations are given in Table I.

In our simulations, the inverter is considered to be connected to the grid via a step-up transformer so that we work with relatively low voltages. The reason for this is to make the simulation

TABLE I
PARAMETERS OF SYNCHRONVERTER

Parameters	Values	Parameters	Values
L_s	0.45 mH	L_g	0.45 mH
R_s	0.135 Ω	R_g	0.135 Ω
C	22 μF	nominal frequency	50 Hz
R (parallel to C)	1000 Ω	nominal voltage (line-line)	20.78 Vrms
rated power	100 W	DC-link voltage	42V

results comparable with the experimental results to be given in the next section. However, the proposed control strategy should work for high voltage and high power as well. We have chosen $D_p = 0.2026$, which means that a frequency drop of 0.5% causes the torque (hence, the power) to increase by 100% (from nominal power). The voltage-drooping coefficient is chosen as $D_q = 117.88$. The time constants of the droop loops are chosen as $\tau_f = 0.002$ s and $\tau_v = 0.002$ s. The simulations were carried out in MATLAB 7.4 with Simulink. The solver used in the simulations was ode23tb with a relative tolerance of 10^{-3} and a maximum step size of 0.2 ms.

The simulation was started at $t = 0$. A PLL was used for the initial synchronization, which will not be discussed in this paper because of page limit. For this reason, the first half-second is omitted from our plots. The initial settings for P_{set} and Q_{set} were zero. The circuit breaker was turned on at $t = 1$ s; the real power $P_{\text{set}} = 80$ W was applied at $t = 2$ s, and the reactive power $Q_{\text{set}} = 60$ Var was applied at $t = 3$ s. The drooping feedbacks were enabled at $t = 4$ s, and then the grid voltage was decreased by 5% at $t = 5$ s.

A. With Nominal Grid Frequency

The system responses are shown in Fig. 5(a). The frequency tracked the grid frequency very well all the time. The voltage difference between v and v_g before any power demand was applied was very small, and the synchronization was very quick. There was no problem turning the circuit breaker on at $t = 1$ s; there was not much transient response caused by this event. The synchronverter responded quickly both to the step change in real-power demand at $t = 2$ s and to the step change in reactive power demand at $t = 3$ s, and it settled down in less than ten cycles without any error. The coupling effect between the real power and the reactive power is reasonably small, and the decoupling control of the real power and reactive power is left for future research. When the drooping mechanism was enabled at $t = 4$ s, there was not much change to the real-power output as the frequency was not changed, but the reactive power dropped by about 53 Var, about 50% of the power rating, because the local terminal voltage v was about 2.5% higher than the nominal value. When the grid voltage dropped by 5% at $t = 4$ s, the local terminal voltage dropped to just below the nominal value. The reactive-power output then increased to just above the setpoint of 60 Var.

B. With Lower Grid Frequency

The simulation was repeated but with a grid frequency of 49.95 Hz, i.e., 0.1% lower than the nominal one. The system responses are shown in Fig. 5(b). The synchronverter followed the grid frequency very well. When the synchronverter worked at the *set* mode, i.e., before $t = 4$ s, the real and reactive power tracked their setpoints with negligible error. After the drooping mechanism was enabled at $t = 4$ s, the synchronverter increased the real power output by 20 W, i.e., 20% of the power rating, corresponding to the 0.1% drop of the frequency. This did not cause much change to the reactive-power output, just a slight adjustment corresponding to the slight change of the local voltage v. The responses in the previous subsection are given in the figure (dashed lines) for comparison.

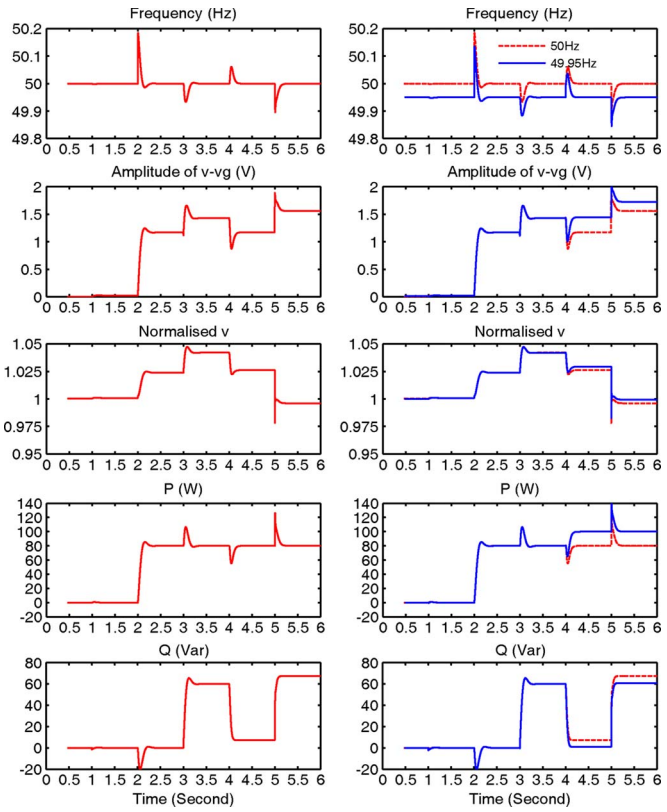

Fig. 5. Simulation results. (a) With the nominal grid frequency. (b) With a lower grid frequency.

VI. EXPERIMENTAL RESULTS

The theory and simulations developed previously were verified on an experimental synchronverter. For safety reasons, this is a low-voltage low-power synchronverter, but it is enough to demonstrate the technology. The parameters of the experimental synchronverter are roughly the same as those given in Table I, and the control parameters are the same. The synchronverter was connected to a three-phase 400-V 50-Hz grid via a circuit breaker and a step-up transformer. The sampling frequency of the controller is 5 kHz, and the switching frequency is 15 kHz. Many experiments were done, but only two typical cases are shown here. The experiments were carried out according to the following sequence of actions:

1) starting the system but keeping all the IGBTs off; using the synchronization algorithm, which is not discussed here;

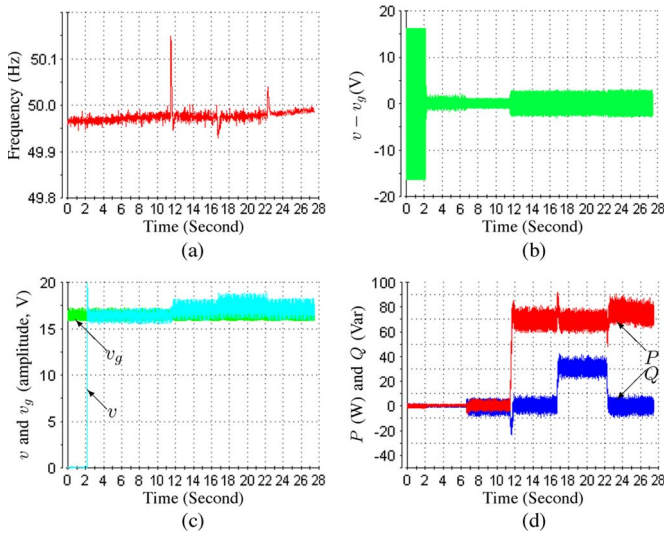

Fig. 6. Experimental results when the grid frequency was < 50 Hz. (a) Synchronverter frequency. (b) Voltage difference. (c) Amplitude of v and v_g. (d) P and Q.

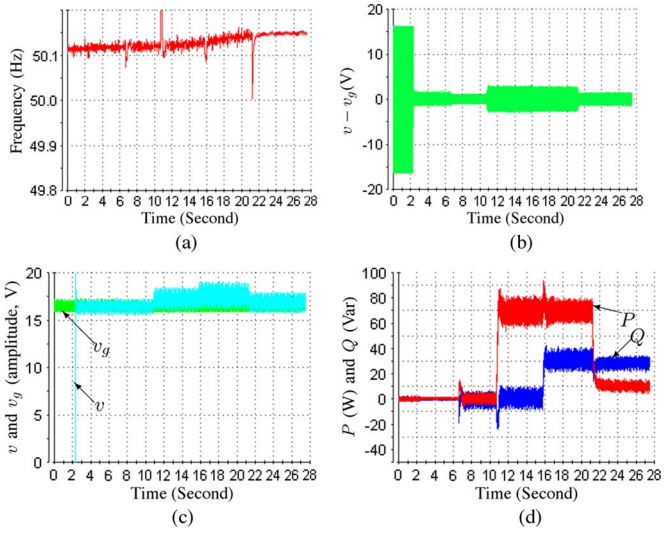

Fig. 7. Experimental results when the grid frequency was > 50 Hz. (a) Synchronverter frequency. (b) Voltage difference. (c) Amplitudes of v and v_g. (d) P and Q.

2) starting operation of the IGBTs, roughly at $t = 2$ s; $P_{\text{set}} = Q_{\text{set}} = 0$;
3) turning the circuit breaker on, roughly at $t = 6$ s;
4) applying $P_{\text{set}} = 70$ W, roughly at $t = 11$ s;
5) applying $Q_{\text{set}} = 30$ Var, roughly at $t = 16$ s;
6) enabling the drooping mechanism, roughly at $t = 22$ s;
7) stopping the data recording, roughly at $t = 27$ s.

A. Case 1: Grid Frequency Was Lower Than 50 Hz

During this experiment, the grid frequency was lower than 50 Hz, increasing from 49.96 to 49.99 Hz. The synchronverter frequency followed the grid frequency very well, with noticeable transients after each action, as shown in Fig. 6(a). The local terminal voltage synchronized with the grid voltage very quickly once the inverter output was enabled, roughly at $t = 2$ s, as shown in Fig. 6(b) and (c). The connection to the grid went very smoothly, and there were no noticeable transients in the frequency or power (see Fig. 6). The power remained around zero but with bigger spikes. After the real-power demand was raised, it took less than ten cycles to reach the setpoint, which is very fast, and the overshoot was very small [see Fig. 6(d)]. This action caused the frequency to respond with a big spike; the synchronverter initially "stored" some reactive power but then released it very quickly. After the reactive-power demand was raised, it took less than ten cycles to reach the setpoint with a small overshoot [see Fig. 6(d)]. The frequency dropped slightly, and the real power increased a bit, but all returned to normal very quickly. Because the drooping mechanism was not enabled, the real power and reactive power delivered by the synchronverter followed the reference values. After the drooping mechanism was enabled, roughly at $t = 22$ s, the synchronverter started to respond to the deviations of the grid frequency and the voltage from their nominal values. The real power delivered was increased as the grid frequency was lower than the nominal value, while the reactive power was decreased as the local terminal voltage was higher than the nominal value.

B. Case 2: Grid Frequency Was Higher Than 50 Hz

During this experiment, the grid frequency was higher than 50 Hz, increasing from 50.11 to 50.15 Hz. There was not much difference from the previous experiment before the drooping mechanism was enabled, except for a slight transient after the connection to the grid, and the synchronverter responded well to the instructions (see Fig. 7). After the drooping mechanism was enabled, roughly at $t = 21$ s, the synchronverter started to respond to the highly deviated grid frequency (0.3%), which meant that the grid had excessive real power and dropped the real-power output by about $0.3\%/0.5\% \times 100 = 60$ to 10 W. The reactive power delivered was decreased slightly as the local terminal voltage was slightly higher than the nominal value, which means that the grid had excessive reactive power.

VII. Conclusion

In this paper, the idea of operating an inverter as an SG has been developed and proved to be feasible after establishing a model for SGs to cover all the dynamics without any assumptions to the signals. The implementation and operation of such an inverter, including power regulation and load sharing, have been developed and described in detail. The mathematical model developed here can be used to investigate the stability of power systems dominated by parallel-operated inverters in distributed generation. Both simulation and experimental results are provided.

Acknowledgment

The authors would like to thank Mr. T. Hornik for his help in preparing the experiments.

References

[1] J. M. Carrasco, L. G. Franquelo, J. T. Bialasiewicz, E. Galvan, R. C. Portillo-Guisado, M. A. M. Prats, J. I. Leon, and N. Moreno-Alfonso, "Power-electronic systems for the grid integration of renewable energy sources: A survey," *IEEE Trans. Ind. Electron.*, vol. 53, no. 4, pp. 1002–1016, Aug. 2006.

[2] S. Busquets-Monge, J. Rocabert, P. Rodriguez, S. Alepuz, and J. Bordonau, "Multilevel diode-clamped converter for photovoltaic generators with independent voltage control of each solar array," *IEEE Trans. Ind. Electron.*, vol. 55, no. 7, pp. 2713–2723, Jul. 2008.
[3] J. Ekanayake, L. Holdsworth, and N. Jenkins, "Control of DFIG wind turbines," *Power Eng.*, vol. 17, no. 1, pp. 28–32, Feb. 2003.
[4] M. Prodanovic and T. C. Green, "Control and filter design of three-phase inverters for high power quality grid connection," *IEEE Trans. Power Electron.*, vol. 18, no. 1, pp. 373–380, Jan. 2003.
[5] C. K. Sao and P. W. Lehn, "Autonomous load sharing of voltage source converters," *IEEE Trans. Power Del.*, vol. 20, no. 2, pp. 1009–1016, Apr. 2005.
[6] K. De Brabandere, B. Bolsens, J. Van den Keybus, A. Woyte, J. Driesen, and R. Belmans, "A voltage and frequency droop control method for parallel inverters," *IEEE Trans. Power Electron.*, vol. 22, no. 4, pp. 1107–1115, Jul. 2007.
[7] T. Loix, K. De Brabandere, J. Driesen, and R. Belmans, "A three-phase voltage and frequency droop control scheme for parallel inverters," in *Proc. 33rd IECON*, 2007, pp. 1662–1667.
[8] P. Piagi and R. H. Lasseter, "Autonomous control of microgrids," in *Proc. IEEE Power Eng. Soc. Gen. Meet.*, 2006. [Online]. Available: http://ieeexplore.ieee.org/stamp/stamp.jsp?tp=&arnumber=1708993
[9] M. Prodanovic and T. C. Green, "High-quality power generation through distributed control of a power park microgrid," *IEEE Trans. Ind. Electron.*, vol. 53, no. 5, pp. 1471–1482, Oct. 2006.
[10] J. M. Guerrero, J. C. Vasquez, J. Matas, M. Castilla, and L. G. de Vicuna, "Control strategy for flexible microgrid based on parallel line-interactive UPS systems," *IEEE Trans. Ind. Electron.*, vol. 56, no. 3, pp. 726–736, Mar. 2009.
[11] J. C. Vasquez, J. M. Guerrero, A. Luna, P. Rodriguez, and R. Teodorescu, "Adaptive droop control applied to voltage-source inverters operating in grid-connected and islanded modes," *IEEE Trans. Ind. Electron.*, vol. 56, no. 10, pp. 4088–4096, Oct. 2009.
[12] "Proposed terms and definitions for flexible AC transmission system (FACTS)," *IEEE Trans. Power Del.*, vol. 12, no. 4, pp. 1848–1853, Oct. 1997.
[13] H.-P. Beck and R. Hesse, "Virtual synchronous machine," in *Proc. 9th Int. Conf. EPQU*, 2007, pp. 1–6.
[14] Q.-C. Zhong and G. Weiss, "Static synchronous generators for distributed generation and renewable energy," in *Proc. IEEE PES PSCE*, Washington, DC, Mar. 2009, pp. 1–6.
[15] J. Driesen and K. Visscher, "Virtual synchronous generators," in *Proc. IEEE Power Energy Soc. Gen. Meeting–Conversion and Delivery of Electrical Energy in the 21st Century*, Jul. 2008, pp. 1–3.
[16] K. Visscher and S. W. H. De Haan, "Virtual synchronous machines (VSG's) for frequency stabilisation in future grids with a significant share of decentralized generation," in *Proc. IET-CIRED Semin. Smart-Grids Distrib.*, Jun. 2008, pp. 1–4.
[17] J. J. Grainger and W. D. Stevenson, *Power System Analysis*. New York: McGraw-Hill, 1994.
[18] A. E. Fitzgerald, C. Kingsley, and S. D. Umans, *Electric Machinery*. New York: McGraw-Hill, 2003.
[19] J. H. Walker, *Large Synchronous Machines: Design, Manufacture and Operation*. Oxford, U.K.: Oxford Univ. Press, 1981.
[20] P. Kundur, *Power System Stability and Control*. New York: McGraw-Hill, 1994.
[21] D. P. Kothari and I. J. Nagrath, *Electric Machines*, 3rd. New Delhi, India: McGraw-Hill, 2004.
[22] A. J. Ellison, *Electromechanical Energy Conversion*. London, U.K.: George G. Harrap Co. Ltd., 1965.
[23] Q.-C. Zhong, J. Liang, G. Weiss, C. M. Feng, and T. C. Green, "H^∞ control of the neutral point in 4-wire 3-phase DC-AC converters," *IEEE Trans. Ind. Electron.*, vol. 53, no. 5, pp. 1594–1602, Oct. 2006.
[24] Q.-C. Zhong, L. Hobson, and M. G. Jayne, "Classical control of the neutral point in 4-wire 3-phase DC-AC converters," *J. Elect. Power Qual. Utilisation*, vol. 11, no. 2, pp. 111–119, 2005.

Qing-Chang Zhong (M'04–SM'04) received the Diploma degree in electrical engineering from Hunan Institute of Engineering, Xiangtan, China, in 1990, the M.Sc. degree in electrical engineering from Hunan University, Changsha, China, in 1997, the Ph.D. degree in control theory and engineering from Shanghai Jiao Tong University, Shanghai, China, in 1999, and the Ph.D. degree in control and power engineering (awarded the Best Doctoral Thesis Prize) from Imperial College London, London, U.K., in 2004, respectively.

He was with the Technion—Israel Institute of Technology, Haifa, Israel; Imperial College London, London, U.K.; and the University of Glamorgan, Treforest, U.K.; and the University of Liverpool, Liverpool, U.K. He is currently with Loughborough University, Leicestershire, U.K. He is the author or coauthor of three research monographs: *Robust Control of Time-Delay Systems* (Springer-Verlag 2006), *Control of Integral Processes with Dead Time* (Springer-Verlag 2010), *Control of Power Inverters for Distributed Generation and Renewable Energy* (Wiley-IEEE Press, scheduled to appear in 2011). His current research focuses on robust and H-infinity control, time-delay systems, process control, power electronics, electric drives and electric vehicles, distributed generation, and renewable energy.

Dr. Zhong is a Fellow of the Institution of Engineering and Technology (Institution of Electrical Engineers) and a Senior Research Fellow of the Royal Academy of Engineering/Leverhulme Trust, U.K. (2009–2010).

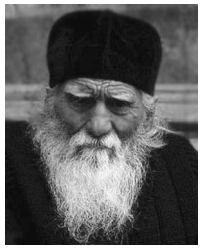

George Weiss received the B.S. degree in control engineering from the Polytechnic Institute of Bucharest, Bucharest, Romania, in 1981, and the Ph.D. degree in applied mathematics from Weizmann Institute, Rehovot, Israel, in 1989.

He was with Brown University, Providence, RI; Virginia Polytechnic Institute and State University, Blacksburg; Weizmann Institute, Ben-Gurion University, Beer Sheva, Israel; the University of Exeter, Exeter, U.K.; and Imperial College London, London, U.K. Currently, he is with Tel Aviv University, Ramat Aviv, Israel. He is a coauthor (with M. Tucsnak) of the book *Observation and Control for Operator Semigroups* (Birkhäuser, 2009). His research interests are distributed parameter systems, operator semigroups, control applied in power electronics, repetitive control, and periodic (in particular, sampled-data) linear systems.